Journal of Solid State Electrochemistry (2018) 22:2889–2900
https://doi.org/10.1007/s10008-018-3992-1

ORIGINAL PAPER

Decolourisation of reactive black-5 at an RVC substrate decorated with PbO_2/TiO_2 nanosheets prepared by anodic electrodeposition

S. Z. J. Zaidi[1] · C. Harito[1] · F. C. Walsh[1] · C. Ponce de León[1]

Received: 1 February 2018 / Revised: 27 April 2018 / Accepted: 10 May 2018 / Published online: 1 June 2018

Abstract

Reticulated vitreous carbon (RVC) substrates were coated with a composite of PbO_2 and titanate nanosheets (TiNS) by anodic electrophoretic depostion. The structure and morphological characteristics of the coating were evaluated by field emission scanning electron microscopy (FESEM) and Raman spectroscopy. The TiNS/PbO_2/RVC coating contained the anatase phase and showed a well-defined, microporous morphology with hydrophilic character along the length and thickness of the RVC struts. Electrochemical and photocatalytic activity of the coatings facilitated RB-5 dye degradation as a model organic pollutant in wastewater. The electrochemical decolourisation involves the generation of hydroxyl free radicals over the TiNS/PbO_2/RVC anode composite surface, whereas photocatalytic decolourisation was driven by the synergetic photocatalytic effect imparted by the photoinduced holes and free electron acceptors. The photocatalytic properties of the TiNS/PbO_2 coating were achieved by calcination at 450 °C for 60 min in air which converted the titanate phase to anatase and modified its surface area. This enabled 98% electrochemical decolourisation of the RB-5 dye solution (measured by visible absorption at 597 nm) in a time of 60 min.

Keywords Anodic electrophoretic deposition · PbO_2 · RVC · TiNS

Introduction

The anodic oxidation of organic compounds in wastewater has attracted great interest due to its ability to purify and clean effluents in a rapid and controlled manner. The methodology has demonstrated high efficiency, especially in research works for pollutant decolourisation and chemical oxygen demand (COD) removal that utilize boron-doped diamond (BDD) electrodes in filter press flow cells [1, 2]. In many cases, however, the application of BDD is limited to laboratory scale, since BDD electrodes are expensive and considerable effort is required to set up a treatment plant. Therefore, there is a need to develop cost-effective coatings, which operate in a similar fashion to BDD and remain stable in a filter press flow cell during the mineralisation, decolourisation, and removal of organic compounds. Over the last decade, TiO_2-based materials and coatings have been adopted as photocatalytic materials with the aid of ultraviolet (UV) light to degrade organic compounds. The increasing interest in electrochemical methods [2], such as electro-Fenton [3], anodic oxidation [4], electrocoagulation [5], solar photoelectro-Fenton [6], and photoassisted electrochemical methods [2], have attracted the attention of researchers in the field of water treatment as efficient, cost-effective, and environmental friendly technologies.

Anodic oxidation has been reported to be effective for partial and complete mineralisation with colour removal of organic compounds by using mixed metal oxides of Ru, Ti, Sb, Sn or Ir, and PbO_2 [7]. Anodic oxidation is widely employed and recognized as much easier in comparison to other electrochemical technologies, such as electrochemical reduction (e.g. direct electrochemical reduction of amaranth azo dye) [2]. Anodic oxidation produces physisorbed hydroxyl radicals $^{\bullet}OH$ that discharge over the anode surface (M) during the electrolysis of water:

$$M + H_2O \rightarrow M(^{\bullet}OH) + H^+ + e^- \quad (1)$$

Highlights • Stable TiNS/PbO_2 films on 100-ppi RVC were achieved by electrophoretic deposition.
• SEM and Raman spectroscopy showed uniform layers of PbO_2/TiNS.
• PbO_2/TiNS/RVC allowed 98% decolourisation of 100-mL RB-5 dye in 60 min.

✉ C. Ponce de León
capla@soton.ac.uk

[1] Electrochemical Engineering Laboratory, Faculty of Engineering and Environment, Engineering Sciences, University of Southampton, Highfield, Southampton SO17 1BJ, UK

The species M(˙OH) react with organic material until mineralisation and produce carbon dioxide and water [4]. Metal oxide electrode material plays an important role during the anodic oxidation reaction, since both chemical reactivity and ability to electrogenerate M(•OH) are related to the nature of the electrode. Different anode materials have been investigated to observe the stability and efficiency in batch as well as flow studies [8–11]. The anode materials should be selected on their high over potential for the oxygen evolution reaction (OER) as well as for their large surface area. On BDD electrodes for example, OER occurs at ca. + 2.3 V vs. SCE and it is more suitable for the production of M(˙OH) species than other materials [12–14].

Titanate nanotube (TiNT) coating has recently emerged as an attractive alternative for wastewater remediation due to their stability at high temperature, ease of preparation, low price, and relatively high oxygen evolution potential of 1.8 V vs. SCE in 0.1-mol L^{-1} Na_2SO_4 solution. For example, TiNT/Sb-doped SnO_2 electrodes showed complete mineralisation and decolourisation for anodic oxidation of benzoic acid at 20 mA cm^{-2} [15]. Other nanomaterials, such as nano PbO_2/TiO_2 and TiO_2 nanosheets, have been used for decolourisation and demineralisation of methyl orange and chloroethene [16, 17]. Recent research has shown that the preparation of PbO_2 anodes decorated with TiO_2 nanotubes was found effective for the complete mineralisation and decolourisation of reactive blue-194 at a current density of 150 mA cm^{-2} [18]. A modified Ti/SnO_2-Sb/PbO_2electrode has also being utilized for the removal of the azo dye acid black-194 at a current density of 30 mA cm^{-2} [19].

Other approaches, seeing to replace expensive metals, such as platinum [20], involve the formation of PbO_2 inside the TiO_2 nanotubes formed on a titanium substrate [21], which show high catalytic activity and large surface areas for electrodegradation. PbO_2 acts as a conductive bridge during the anodic oxidation [22] demonstrating their suitability as electrodes for wastewater treatment [23, 24].

PbO_2 coatings on RVC or a carbon-polymer substrate obtained by electrodeposition in methanesulfonic acid electrolytes have been found effective for electrochemical water treatment [25]. The inclusion of TiNT films has been claimed to be 100% efficient for the mineralisation and removal of benzoic acid from wastewater [15]. The anatase phase of TiNT provides active surface area of 20 m^2 g^{-1}, larger than the traditional Degussa P25 TiO_2 particles that have a 7-m^2 g^{-1} surface area and are 20% more efficient for the photo decolourisation of rhodamine-B dye [26]. The potential advantage of using a substrate with defined regular structure, such as RVC, provides efficient mass transport of the effluent over the surface, which ultimately provides efficient degradation [27]. RVC possesses a honeycomb structure [28] and has been employed for the electro Fenton degradation of azo dyes [1].

Polypyrrole/anthroquinone disulphonate composite film-modified graphite cathodes were used for the oxidation of azo dyes and achieved up to 80% mineralisation by electro-Fenton [29]. RVC was also employed to produce hydrogen peroxide to form the Fenton reagent and oxidase formic acid [30] and for removing metal ions [31, 32]. RVC substrate coated with TiNT produced inexpensive novel electrodes for advanced processes, such as anodic oxidation and photocatalytic degradation. In another example, TiO_2 nanotubular arrays and titanium-based electrodes have showed considerable electrocatalytic behavior of organic compounds like ascorbic acid, glucose, dopamine, and alcohols [33, 34]. The use of lower cost carbonaceous alternatives, such as carbon foam PbO_2 composite coatings with TiNT, is worth study due to their morphology and porosity, which increase the stability of TiNT during anodic oxidation [35].

The inclusion of photocatalytically active titanium dioxide produces electron-hole pairs, as depicted in reaction (2), under UV light.

$$TiO_2 + UV \rightarrow e^-_{CB} + h^+_{VB} \quad (2)$$

The adsorbed photons over the titanium dioxide nanoparticulate photocatalyst are initiated at an energy greater than 3.2 eV, which corresponds to the energy necessary to excite an electron from the valance to the conductive band with the formation of positive hole at the valance band [36]. This creates electron-hole pairs, and the active electrons can form superoxide ions $\left(O_2^{-\bullet}\right)$ and peroxide radicals by reacting with O_2 as shown in reactions (3) and (4) [37, 38].

$$e^-_{CB} + O_2 \rightarrow O_2^{-\bullet} + H^+ \quad (3)$$

$$O_2^{-\bullet} + H^+ \rightarrow HO_2^- \quad (4)$$

Such photocatalysis is reported in the literature for TiO_2 under UV light irradiation [39]:

$$2HO_2^- \rightarrow H_2O_2 + O_2^- \quad (5)$$

$$H_2O_2 + O_2^{-\bullet} \rightarrow {}^{\bullet}OH + OH^- + O_2 \quad (6)$$

$$H_2O + h^+_{VB} \rightarrow {}^{\bullet}OH + H^+ \quad (7)$$

Reaction (5) involves production of hydrogen peroxide, while reactions (6) and (7) represent the formation of •OH radicals. The oxidation of a water molecule forms the short-lived and powerful oxidant •OH radical (redox potential = 2.7 V vs. SCE) [40]. This oxidant is capable of decolourisation and mineralising organic matter residue to lower molecular weight compounds and ultimately to carbon dioxide and water [41].

The aim of this study is to investigate the electrochemical and photochemical performance of TiNS/PbO_2 coating on RVC for the decolourisation of reactive black-5 (RB-5) dye and characterize the structural and morphological properties

of the coatings. The decolourisation of this dye is important due to its widely commercial usage in the leather, wool, polymer, rubber, and silk industries.

Experimental details

Reagent grade 50% Pb (II) methanesulfonate ($Pb(CH_3SO_3)_2$, 70% methanesulfonic acid (MSA), tetrabutylammonium hydroxide (TBAOH), cesium carbonate (Cs_2CO_3), Degussa TiO_2 (P25), and reactive black-5 (RB-5) dye were purchased from Sigma Aldrich, while hydrochloric acid, sulfuric acid, sodium hydroxide, sodium sulphate, and acetone obtained from Fischer scientific and used as received.

Synthesis of titanate nanosheets

A single-layer of titanate nanosheets (TiNS) was developed using an adapted methodology from Sasaki et al. [42]. TiNS were prepared by the solid reaction between the Cs_2CO_3 and P25 at molar ratio 1:5.3 and 800 °C for 90 min. Once cooled, the resultant mixture was ground into fine powder. The powder was reheated at 800 °C for two cycles of 20 h each; after each interval of high-temperature treatment, the resulting mixture was cooled overnight and ground to fine powder. The resulting white powder was lepidocrocite-like cesium titanate, $Cs_{0.7}Ti_{1.82}\square_{0.175}O_4$, where □ represents a vacancy [43].

Ion exchange method was used to produce smectite-like acid titanate from a mixture that contained 2 g of lepidocrocite-like cesium titanate and 80 mL of 1-mol L^{-1} HCl. The solution was stirred with a magnetic follower over 4 days at 700 rpm. The solution was replaced with a fresh acid solution every day to maintain the amount of H^+ ions at 1 mol L^{-1} for acid leaching of Cs^+ ions. The remaining solution was vacuum filtered by employing a nylon membrane and ultimately cleaned with distilled water until the conductivity reached around 10 μS cm^{-1}. The resulting smectite-like acid titanate was recovered and used to produce exfoliated single-layer TiNS. This was achieved by stirring 0.4 g of smectite-like acid titanate with 100 mL of aqueous solution of 0.0165-mol L^{-1} tetrabutylammonium hydroxide (TBAOH) at 200 rpm and room temperature (25 °C) for 2 weeks. This process replaced the protons (H^+) present in the TiNS with bulky (TBA^+) ions. The exfoliated nanosheets were obtained as an aqueous suspension.

Electrodeposition of PbO_2 on RVC

A piece of RVC substrate from ERG materials of 100 pores per linear inch (ppi, porosity grade of RVC) of 2-cm × 2-cm × 0.15-cm dimensions was treated with 70% nitric acid (Fisher Scientific) at 110 °C for 1 h and thoroughly rinsed and left in deionized water overnight, then dried at 90 °C overnight. A Cu wire was glued (Leit-C, Agar scientific) to the RVC to provide electrical connection. The RVC electrode was placed in an undivided electrochemical glass cell fitted with a water jacket connected to a water thermostat, Grant LT D6G model (Fig. 1), and was surrounded by a cylindrical mesh of stainless steel to provide uniform potential distribution. The cell was filled with an electrolyte solution containing 1-mol L^{-1} $Pb(CH_3SO_3)_2$ and 0.2-mol L^{-1} MSA 100 mL of electrolyte. The electrodeposition of PbO_2 on the RVC anode was carried out at 2.5 A at 60 °C for 30 min with a constant stirring of electrolyte at 700 rpm with a 0.25-cm long PTFE-coated magnetic follower [44, 45].

Anodic electrophoretic deposition

The RVC substrate coated with PbO_2 was used as an anode for the electrophoretic deposition of TiNS from a solution containing exfoliated TiNS with TBAOH. The cathode was graphite plate of 1.5-cm × 6-cm × 1.2-cm dimensions in a parallel plate configuration with an interelectrode gap, *d*, of 1 cm. A cell potential difference of 15 V was applied between the electrodes, which created a potential gradient of 15 V cm^{-1}. The electrolyte was vigorously stirred at 700 rpm with a magnetic stirrer, as shown in Fig. 2.

Heat treatment

The TiNS/PbO_2/RVC samples obtained from electrophoretic deposition were calcined at 450 °C for 1 h. The sections of RVC that were not coated with TiNS/PbO_2 film due to the fact that material outside the electrolyte, disintegrated at such a high temperature, whereas those coated with the film resisted calcination. The TiNS film calcined after the heat treatment exhibited uniform coating over the RVC substrate.

Characterisation of the coated substrate

The surface morphology of the TiNS/PbO_2/RVC samples was characterized by field emission scanning electron microscope (FESEM), using a JEOL 6500F at an accelerating voltage of 20 kV. Raman spectra were obtained using a confocal microscope (Renishaw, RM 2000) fitted with a light source of 632.8-nm wavelength to measure the peaks for the presence of deposited species. The exposure time was 30 s with a 10% intensity of laser radiation.

Electrochemical experiments

The electrochemical experiments were performed by means of a computer aided PGSTAT302 N potentiostat/galvanostat from Autolab (EcoChemie, Netherlands) by using Nova 1.11 software. The obtained coatings including calcined TiNS/PbO_2/RVC, PbO_2/RVC, and acid treated RVC were washed with ultra-pure water and dried. Each electrode was used to electrolyze a solution of 100 mL containing 10 ppm of

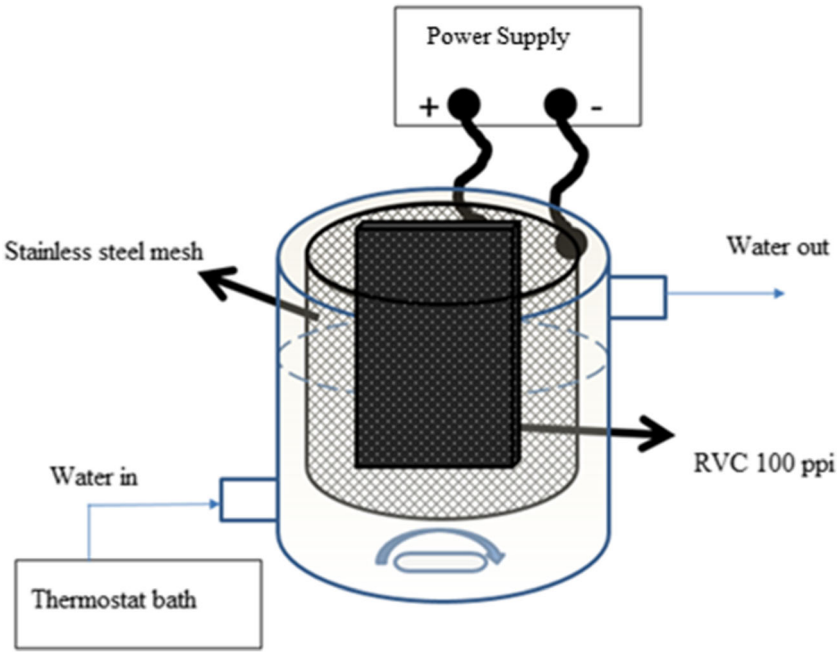

Fig. 1 Electrodeposition of PbO_2 from a solution containing 1-mol L^{-1} Pb $(CH_3SO_3)_2$ and 0.2-mol L^{-1} MSA at 2.5 A and 60 °C for 30 min in a small undivided glass cell containing 100 mL of electrolyte with constant stirring at 700 rpm

RB-5 dye in 0.5 mol L^{-1} of sodium sulphate at pH = 3 and 25 °C at 2 mA cm^{-2}. The electrolyte was stirred and maintained a stable pH throughout the electrochemical studies. Platinum mesh and Hg/HgO (0.6-mol L^{-1} NaOH) were used as a counter and reference electrodes, respectively.

Photocatalytic experiments

The calcined TiNS/PbO_2/RVC sample was cut into a disc of 4-mm diameter and 2-mm thickness (0.919 g) and was fitted in a glass tube holder which was immersed in a 10-mL solution containing 10 ppm of RB-5 dye in 0.5 mol L^{-1} of sodium sulphate at pH 3 in Fig. 2b). The photocatalytic experiments were performed under a UV lamp with 20-mW cm^{-2} intensity. Prior to the photocatalytic experiments, the solution with tube holder was kept in the dark for 30 min in order to achieve maximum adsorption of RB-5 dye on the calcined TiNS/PbO_2/RVC. This ensured that the decolourisation measurements in solution were due to the UV irradiation and not to the adsorption of the dye on the composite. Following this, the UV irradiation was provided every 1 min to the solution. The absorbance of the RB-5 in solution was measured in a Hitachi U3010 UV-Vis spectrophotometer at a wavelength of 597 nm. A calibration curve was used to evaluate the concentration of RB-5 dye in the solution.

Results and discussion

Surface characterisation of TiNS/PbO_2 coated RVC

Figure 3a shows PbO_2 layer coated over the strut of the 100-ppi RVC after electrodeposition at 2.5 A, whereas Fig. 3b shows the micrograph image of the PbO_2 agglomerates covering the surface of RVC at larger magnification. TiNS films were anodically deposited on the PbO_2/RVC surface by electrophoretic deposition as seen in Fig. 3c, which provides more uniform morphology than the PbO_2/RVC film. The more magnified SEM image as seen in Fig. 3d revealed the presence of smooth and elongated strands of TiNS on the top of the PbO_2/RVC. The TiNS/PbO_2/RVC coating covers the typical tetrahedron structure of the RVC (100 ppi) substrate. The high resolution image (30,000 magnification) of TiNS/PbO_2/RVC coating exhibit that TiNS are nanosize particles distributed over the substrate.

After calcination at 450 °C, the TiNS/PbO_2/RVC coatings remain stable as shown in Fig. 4a. The high temperature of the calcination creates surface defects over the TiNS/PbO_2/RVC coatings. The image also shows that the nanosheets are still attached to the PbO_2/RVC coating even after the calcination at 450 °C.

Figure 4b is an image obtained for similar coating, which denotes an undulated surface with ridges and valleys of TiNS/PbO_2/RVC coatings after the transformation of the TiNS from the titanate to the anatase phase which imparts the photocatalytic active nature to the film and can be used to degrade reactive black-5 dye. The uncoated RVC (used to connect to the power supply during electrodeposition) oxidised at high temperature, while the carbon on the coated areas remained intact, which suggests that TiNS/PbO_2 coating preserves the mechanical integrity of the RVC structure.

The elemental analysis of the coating was determined by EDX from the micrograph shown in Fig. 5a. It confirmed that the TiNS/PbO_2/RVC coating contained titanium, lead, and carbon elements. Figure 5b–d shows the elemental maps revealing particles uniformly distributed over the substrate.

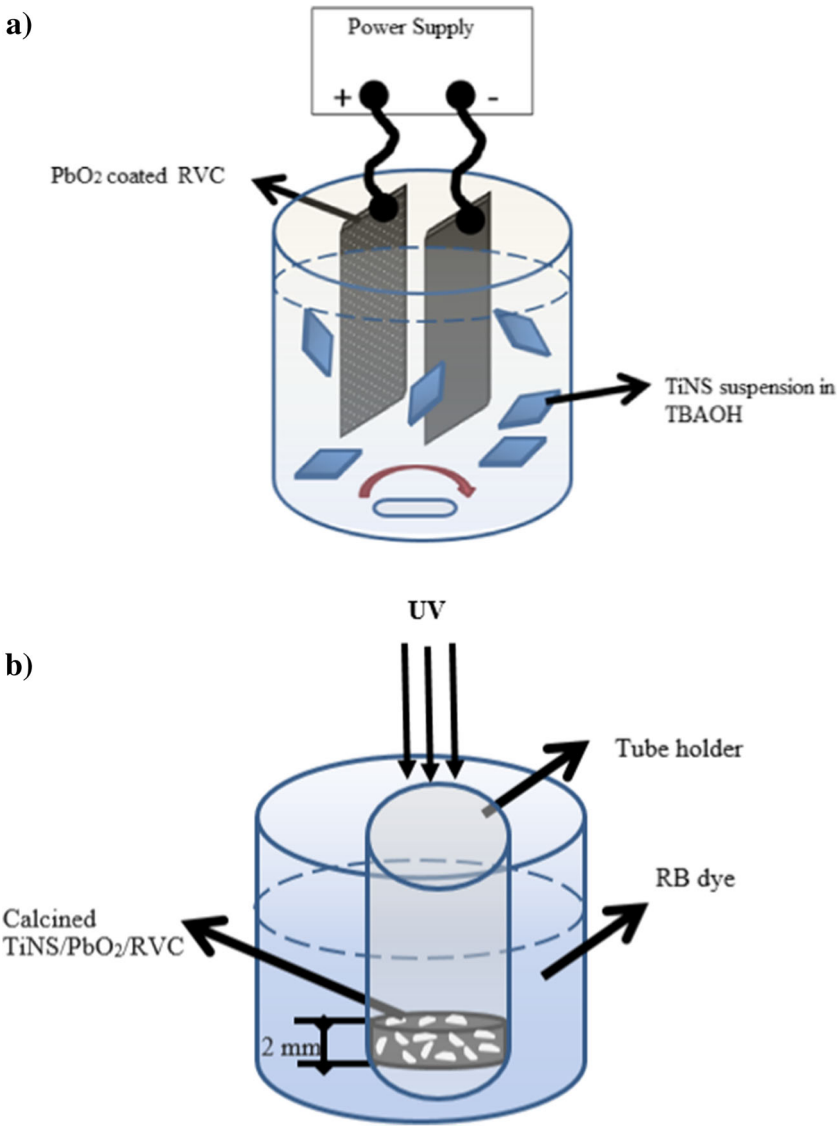

Fig. 2 **a** Schematic diagram of cell for deposition of TiNS suspension containing 100 mL of TiNS exfoliated with tetrabutylammonium hydroxide (TBAOH) at 25 °C. **b** Schematic diagram of the arrangement for photocatalytic decolourisation of the dye

The structural characteristics related to the transformation of the TiNS after the heat treatment were seen by Raman spectroscopy as shown in Fig. 6. The peaks seen at 177, 200, 397, 517, 639, and 747 cm^{-1} in the curve a indicate that heat treatment converted the film from titanate to anatase phase, which have been previously reported in the literature [46]. The peaks observed at 279 and 464 cm^{-1} in curve b for non-calcined coatings disappeared after calcination.

Electrochemical studies of the coatings

The OER is an unwanted reaction during the direct electrochemical anodic oxidation of organic compounds. The first step is the formation of hydroxyl radical ($^{\bullet}OH$) from the water oxidation at the anode substrate (Eq. (1). The following steps depend upon the nature of electrode substrate. Two types of substrates can be classified for direct anodic oxidation: "active" and "non-active" electrodes [4]. In active anodes, strong interaction of the hydroxyl radicals over electrodes takes place due to oxides generation [2], which leads to the OER (4). Platinum is as an active anode, as it is capable of attracting hydroxyl radicals over its surface, due to its greater adsorption enthalpy. In the case of non-active electrodes like PbO_2, there is weak interaction of the electrodes with hydroxyl ($^{\bullet}OH$) radicals which are more prone to react in the electrolyte and oxidise organic compounds dissolved in solution [8].

Cyclic voltammetry studies using calcined TiNS/PbO_2/RVC and PbO_2/RVC electrodes in 0.5-mol L^{-1} Na_2SO_4 at a scan rate of 10 mV s^{-1} are shown in Fig. 7a. The electrode potential at which the OER starts to be significant (> 1 mA cm^{-2}) on the calcined TiNS/PbO_2/RVC, (curve 1) was 2.2 V vs. Hg/HgO, whereas in the case of PbO_2/RVC, curve 2, the oxygen evolution started at > 1.8 V vs. Hg/HgO. The higher overpotential for the OER observed in calcined TiNS/PbO_2/RVC suggests that this coating can potentially be a better catalyst for the production of hydroxyl radicals.

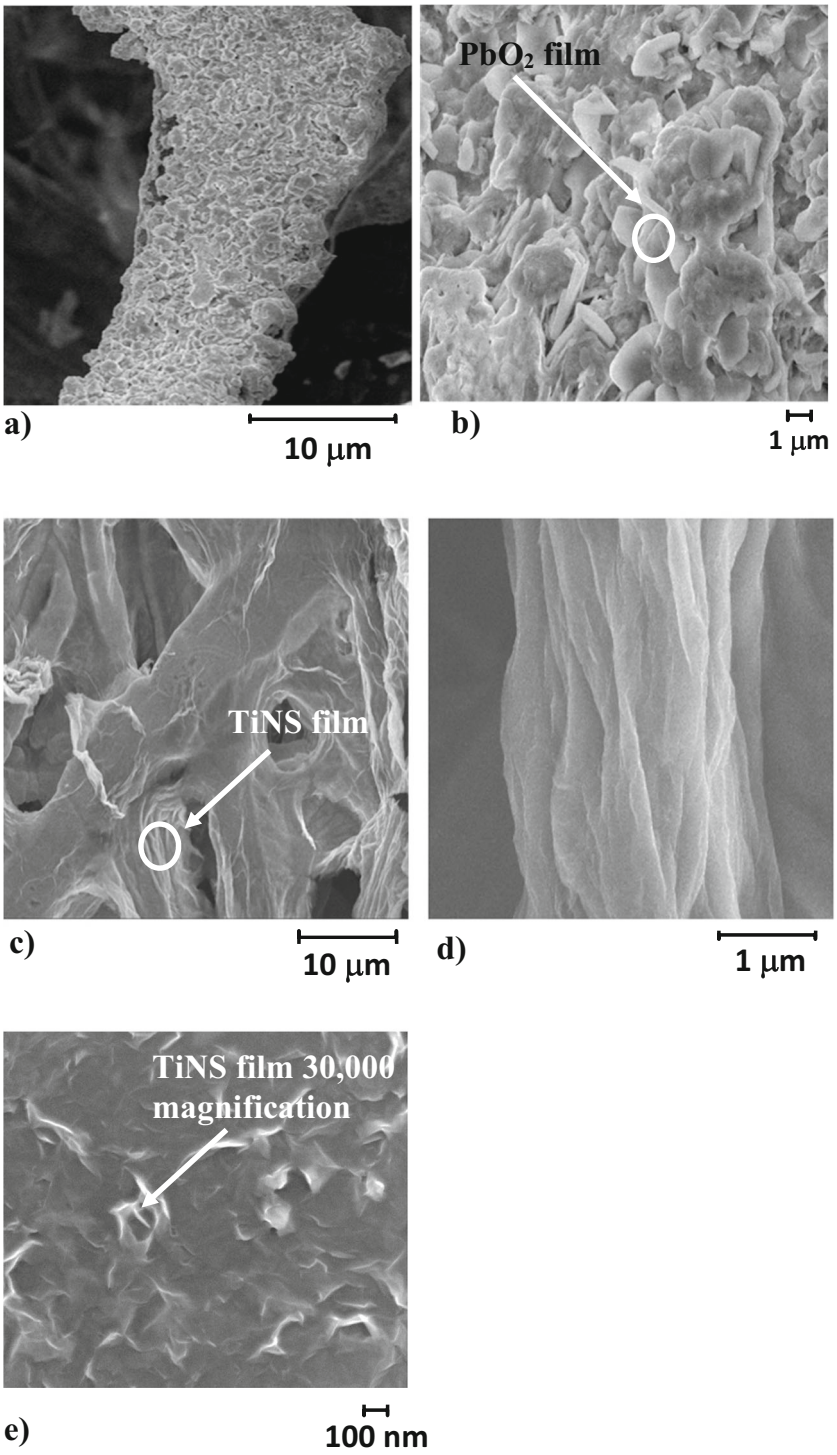

Fig. 3 FESEM images of TiNS/PbO_2 coatings over the RVC substrate obtained by electrodeposition and anodic electrophoretic deposition. **a** RVC strut coated with PbO_2 after anodic electrodeposition. **b** PbO_2 film at higher magnification. **c** TiNS/PbO_2/RVC layer showing fully covered layer of TiNS film over PbO_2/RVC. **d** TiNS/PbO_2/RVC layer at higher magnification. **e** TiNS/PbO_2/RVC at 30,000 magnification at a scale of 100 nm

When 10 ppm of RB-5 dye was added to the solution of 0.5-mol L^{-1} Na_2SO_4, the oxidation process on the calcined TiNS/PbO_2/RVC started earlier at around 0.5 V vs. Hg/HgO but the current was around 1 mA cm^{-2} at 1.4 V vs. Hg/HgO. This suggests that the oxidation of the dye on this catalyst started before the OER as can be seen in Fig. 7b (curve 1). In the case of the PbO_2/RVC electrode (curve 2), no significant oxidation of the dye was observed in comparison to curve 1 and the current density observed is significantly higher than the calcined TiNS/PbO_2/RVC after 2.5 V vs. Hg/HgO. This might be due to the fact that by increasing the potential, the formation of the hydroxyl radical ($^{\bullet}OH$) competes with the direct oxidation of the dye and this oxidation is undetectable due to lower current density recorded in the voltammograms [10, 44].

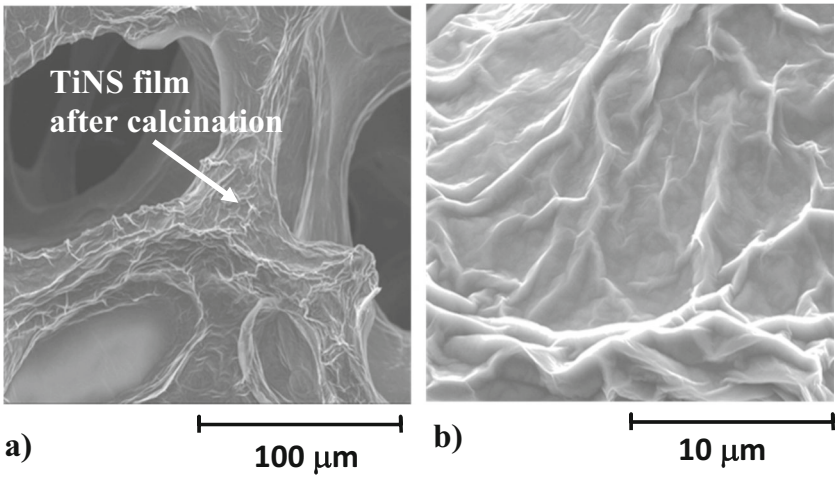

Fig. 4 **a** TiNS/PbO_2/RVC after calcination at 450 °C. **b** Calcined TiNS/PbO_2/RVC layer having undulated surfaces at higher magnification

Electrochemical decolourisation and colour removal of RB-5 dye

Electrolysis at constant current of 2 mA cm^{-2} was carried out in order to remove the colour from the RB-5 dye solutions using different coatings. The electrolyte consisted of 100 mL of solution containing 10 ppm of RB-5 dye in 0.5-mol L^{-1} Na_2SO_4 at pH 3. UV-Vis spectra were used to follow the colour removal of RB-5 dye, which shows a maximum absorption band in the visible light region at λ_{max} = 597 nm. The oxidation of the azo dye complex molecule leads to low molecular weight intermediates, such as aliphatic and aromatic organic molecules [4]. The formation of these compounds is due to the displacement of the chromophore functional group and followed by the oxidation of the organics to carbon dioxide and organic acids (carboxylic acids) [19–21].

The time-dependent profiles of the normalized concentration c/c_o, for the electrochemical decolourisation of the dye using RVC, PbO_2/RVC, and calcined TiNS/PbO_2/RVC anode electrodes are shown in Fig. 8. The data of the concentration decay for the decolourisation of RB-5 dye on different electrodes can be fitted into the following logarithmic relationship:

$$\ln\left(\frac{c}{c_0}\right) = -kt \tag{7}$$

where k is the rate constant, c the concentration, and t the reaction time. The fitting suggests a pseudo-first-order reaction kinetics for the decolourisation. The comparison of rate constant (k) is presented in Table 1.

It can be seen that the pseudo-first-order rate constant decolourisation kinetics obtained using different anodes and from the data from the literature depends upon the nature of the electrocatalytic activity of the coating [40]. The anode electrodes utilized are able to decolourate the solution < 99% except for RVC electrode. This may be due to the tendency of PbO_2/RVC and calcined TiNS/PbO_2/RVC anodes to utilize $^{\bullet}OH$ radicals produced from water discharge reaction and

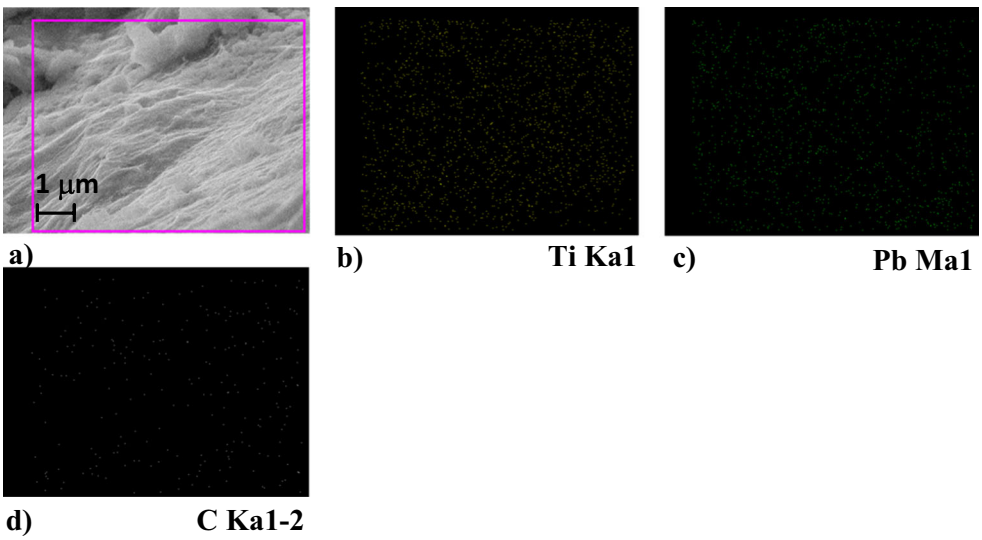

Fig. 5 EDX images for elemental analysis of calcined TiNS/PbO_2/RVC obtained by anodic electrophoretic deposition. **a** Calcined TiNS/PbO_2/RVC. **b** Titanium elemental analysis. **c** Lead elemental analysis. **d** Carbon (RVC) elemental analysis

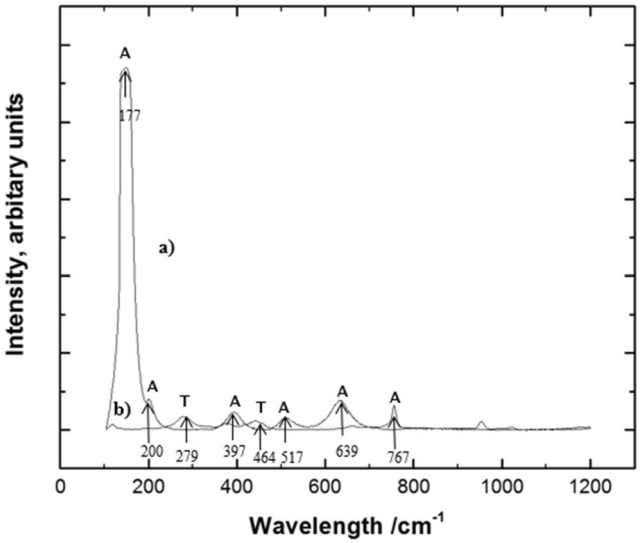

Fig. 6 Raman spectra of the TiNS/PbO_2/RVC obtained by anodic electrophoretic deposition **a** calcined at 450 °C and **b** non-calcined

employ the radicals for the decolourisation of organic dye as shown in Eq. (8) below:

$$\mathrm{RB{-}5} + {}^{\bullet}\mathrm{OH} \rightarrow \mathrm{Intermediates} \rightarrow \mathrm{H_2O} + \mathrm{CO_2} \tag{8}$$

The generation of hydroxyl radicals for the decolourisation of dyes over active electrodes plays an important part; however, they are also part of the mechanism to generate oxygen. If the OER is favored, the decolourisation of organics will be compromised [5]. In order to avoid this competition, the electrodes with large overpotential for oxygen evolution like TiNS/PbO_2/RVC and PbO_2/RVC are preferred. The logarithm of the normalized concentration of RB-5 decay vs. time when a current density of 2 mA cm^{-2} was applied on the anodes is shown in Fig. 9. The comparison of these electrodes shows that using TiNS/PbO_2/RVC removes 98% of the colour with linear pseudo-first-order decolourisation and rate constant $k = -0.060$ min^{-1}.

Colour removal is also substantial when using PbO_2/RVC electrode as shown by the normalized concentration data in Fig. 9, which is around 98%. This behavior is due to the production of Pb ($^{\bullet}$OH) as explained in Eq. (1) [41]. Negligible decolourisation results were obtained in case of RVC alone, which were about 36% colour removal after 60 min which is lower compared to the previously mentioned electrodes. Some reported works showed only 70% conversion of RB-5 dye by using photoassisted Fenton, which is lower than the values reported here [47]. This revealed that the $^{\bullet}$OH radical is weakly adsorbed over the surface of non-active electrode (PbO_2) [8] and ultimately favors the production of $^{\bullet}$OH radical as indicated in Eq. (1) and also subsequent adsorption of the dye molecules over the active sites provided by positively charged TiNS under acidic conditions over the PbO_2/RVC substrate.

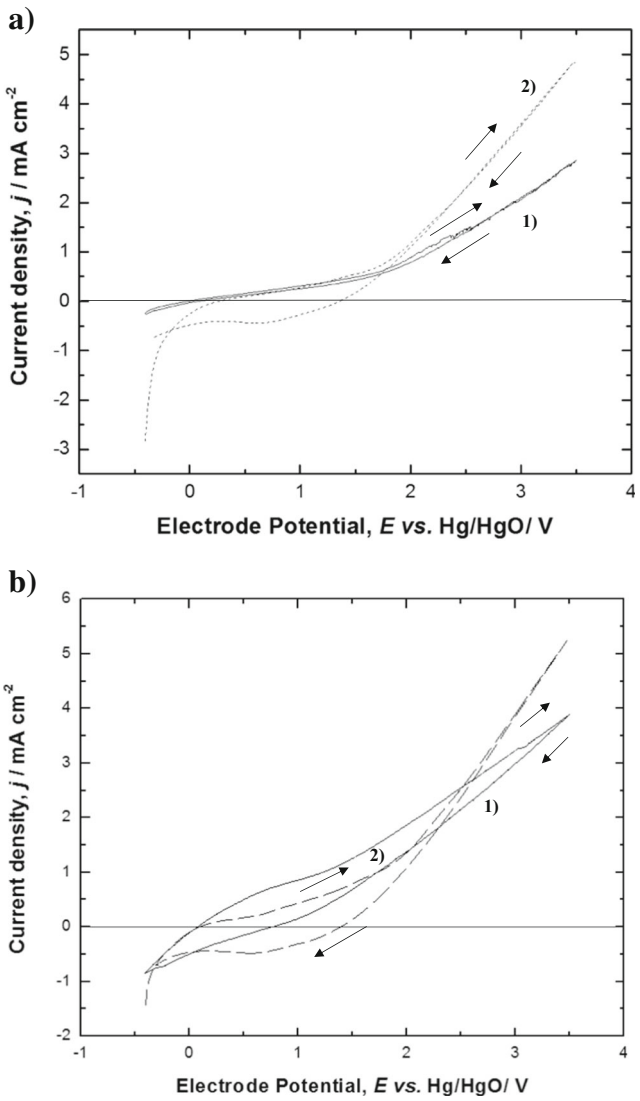

Fig. 7 **a** Polarisation curve by using coating 1 (TiNS/PbO_2/RVC) as anode after calcination at 450 °C in 0.5-mol L^{-1} Na_2SO_4, pH = 3.0. 2) (PbO_2/RVC) as anode in 0.5-mol L^{-1} Na_2SO_4. Experimental conditions: potential sweep rate 10 mV s^{-1}, temperature 298 K. **b** Polarisation curve by using novel coating 1 (TiNS/PbO_2/RVC) as anode in an electrolyte 10-ppm R.B-5 dye in 0.5-mol L^{-1} Na_2SO_4, pH = 3.0. 2) (PbO_2/RVC) as anode after calcination at 450 °C in an electrolyte 10-ppm R.B-5 dye in 0.5-mol L^{-1} Na_2SO_4, pH = 3.0, Experimental conditions: potential sweep rate 10 mV s^{-1}, temperature 298 K

Photocatalytic decolourisation of RB-5 dye

In order to evaluate the photocatalytic activity of the anatase phase of the calcined TiNS (TiO_2)/PbO_2/RVC coating characterized by Raman studies (Fig. 6), photocatalytic studies of the decolourisation of RB-5 dye in Na_2SO_4 and pH = 3 were carried out. The coating showed noticeable photocatalytic activity towards decolourisation of RB-5 dye. The activity of the coating depends on factors like protonation of TiO_2 nanosheets in acidic media [53] and the generation of holes and electrons over the nanosheet surface in the presence of UV

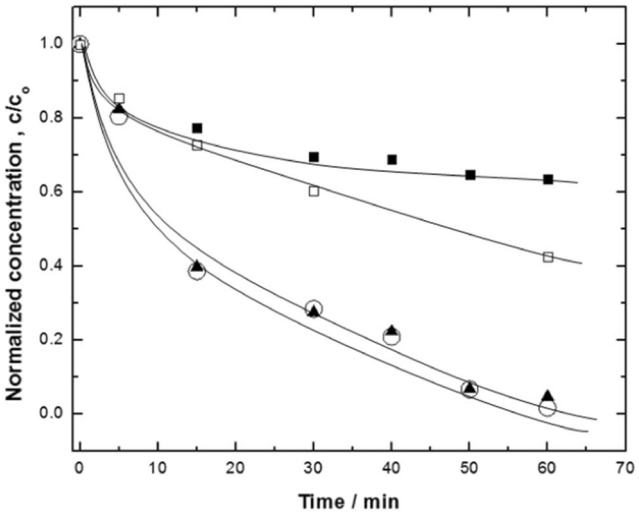

Fig. 8 Electrochemical remediation of RB-5 dye by (■) RVC, (□) photoassisted Fenton using iron oxide on activated alumina support [47], (▲) RVC/PbO_2, and (○) calcined TiNS/PbO_2/RVC

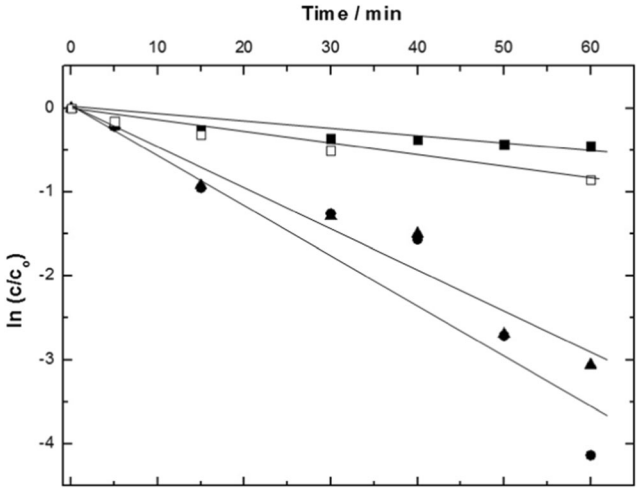

Fig. 9 Electrochemical remediation kinetics of RB-5 dye by (■) RVC, (▲) RVC/PbO_2, and (●) calcined TiNS/PbO_2/RVC

irradiation [54, 55]. In acidic solutions, the TiO_2 nanosheets become positively charged as indicated by Eq. (10) and attract the negatively charged RB-5 dye [49].

$$TiOH + H^+ \rightarrow TiOH_2^+ (\text{acidic solution}) \quad (10)$$

Under UV light, there is the formation of electrons (e^-) in the conduction band and holes (h^+) in the valance band of the TiO_2 nanosheet anatase as seen in Eq. (11). The photo-induced holes possess oxidative properties, which can attack the dye molecule directly leading to its decolourisation or indirectly forming hydroxyl radicals by promoting the reaction between the hydroxyl anions and water as shown by Eq. (12). The hydroxyl radicals react with the organic matter. However, the electrons can also react with an electron acceptor like O_2 to produce oxidizing radicals $O_2^{-\bullet}$ as shown by reaction (13) [49].

$$TiO_2 + h\nu \rightarrow e^-_{CB} + h^+_{VB} \quad (11)$$

$$OH^- + h^+_{VB} \rightarrow {}^\bullet OH + H^+ \quad (12)$$

$$e^-_{CB} + O_2 \rightarrow O_2^{-\bullet} \quad (13)$$

$$RB{-}5 + {}^\bullet OH \rightarrow \text{Decompose} \quad (14)$$

Overall, the holes and radicals are responsible for the photocatalytic activity and decolourisation of RB-5 dye as indicated by Eqs. (4), (5), and (6) producing $^\bullet OH$ radical, which ultimately decompose the dye as shown in Eq. (14). In this case, PbO_2 dominates the base of the conduction band of TiNS (anatase TiO_2), while the valance band belongs to the TiNS (anatase TiO_2) nanoparticle states [56]. The formation of the new band gap will intensify the electron-hole pair transfer

Table 1 Comparison of apparent rate constants for decolourisation of RB-5 dye by RVC, calcined TiNS (TiO_2)/PbO_2/RVC, and PbO_2/RVC and other related values from selected literature

Substrate	$-k$/min^{-1}	Decolourisation %	Time/min	Reference
RVC by using anodic oxidation	0.0064	36	60	This study
PbO_2/RVC by using anodic oxidation	0.050	97	60	This study
Calcined TiNS(TiO_2)/PbO_2/RVC by using anodic oxidation	0.060	98	60	This study
Calcined TiNS(TiO_2)/PbO_2/RVC by using photocatalytic decolourisation	0.383	85	5	Photocatalytic rate in this study
TiO_2 (P25) by using photocatalytic degradation	0.038	≈ 90	60	[48]
TiO_2 nanofiber-nanoparticle composite by using photocatalytic degradation	0.039	94.4	60	[49]
TiO_2 nanofiber composite by using photocatalytic degradation	0.026	75.5	60	[50]
Photoassisted Fenton by using iron oxide on activated alumina support	N.G	70	480	[47]
TiO_2-P25 by using photocatalytic degradation	N.G	98	150	[51]
UV/H_2O_2 by using Iron salt	N.G	99.3	180	[52]

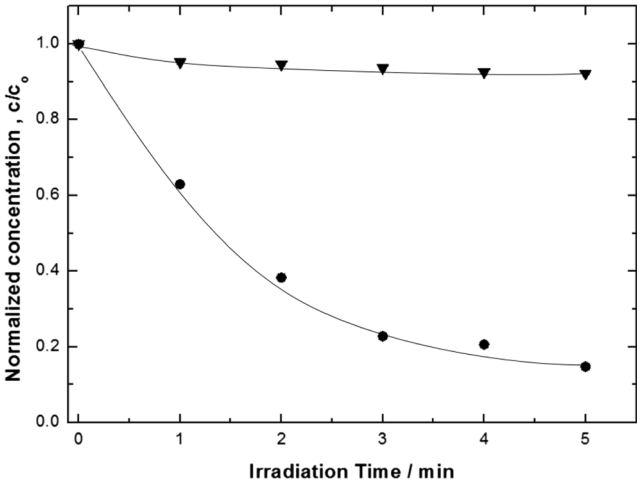

Fig. 10 Photocatalytic remediation of RB-5 dye by (▼) RVC, (●) calcined TiNS/PbO_2/RVC, (■) using calcined TiNS/PbO_2/RVC

upon photoexcitation. The photocatalytic decolourisation is shown in Fig. 10 and indicates that the RB-5 dye follows a pseudo-first-order reaction kinetics on the calcined TiNS/PbO_2/RVC coating, as revealed in Fig. 11.

The comparison of rate constant (k) calculated by using Eq. (7) for the photocatalytic decolourisation ($-0.383\ min^{-1}$) with electrochemical decolourisation ($-0.060\ min^{-1}$) reveals that photocatalytic activity is higher by 84%. The annealing converts TiNS to the single-crystal anatase phase, which improved the photocatalytic activity when irradiated with UV light. The calcined TiNS/PbO_2/RVC decolourized the reactive black-5 solution in 15 min. The improved photocatalytic activity of a coating, i.e. TiNS/PbO_2/RVC ascribed due to the formation of holes and radicals by the incident UV light and ultimately participates in the photocatalytic decolourisation of the dye.

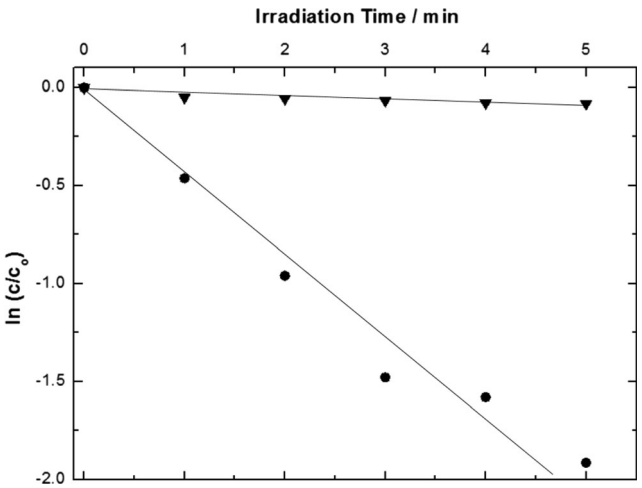

Fig. 11 Photocatalytic remediation kinetics by (▼) RVC, (●) calcined TiNS/PbO_2/RVC

Conclusions

Lead dioxide was electrodeposited on RVC, and the resulting coating decorated with TiNS was firstly prepared via anodic electrophoretic deposition followed by calcination.

The following are the main findings:

- Compared with RVC alone and PbO_2/RVC electrodes, the calcined TiNS/PbO_2/RVC coatings were able to decolourise RB-5 dye from wastewater more effectively.
- The calcined TiNS/PbO_2/RVC was also found effective for the photocatalytic decolourisation of the dye.
- The nature of the electrode plays an important part in decolourisation and colour removal of the organic chromophore in the dye. The hydroxyl free radical ($^{\bullet}OH$) generates on the electrode surface provides an efficient and clean method for the decolourisation of RB-5 dye. Using calcined TiNS/PbO_2/RVC electrodes; a first-order decolourisation kinetics has been determined with higher rate of reaction in comparison with some reported values in the literature.
- Raman results indicated the transformation of the titanate phase of TiNS/PbO_2/RVC to the anatase structure after calcination at 450 °C.
- The anatase phase in the coating also found effective in photocatalytic studies and removal results revealed a first-order kinetics decolourisation of RB-5 dye in acidic conditions.
- The photocatalytic effect resulted from three mechanisms, which involve photoinduced holes in valance band, the protonation of TiNS in acidic solutions, and the formation of oxidative radicals evolved from the reaction between the electrons from the conduction band and the electron acceptor ($^{\bullet}O_2$).

This study opens up a promising approach in developing metal oxide structures decorated with TiO_2 nanosheets over inexpensive carbon based substrate, for applications in wastewater treatment. TiNS coating on RVC also improved thermal resistance of RVC. Therefore, these coatings could potentially serve the purpose of decontamination of wastewater by using cheaper and flow-through electrodes such as RVC with the combination of PbO_2 and TiNS.

Acknowledgements S.Z.J. Zaidi is grateful to the Faculty of Engineering and the Environment at the University of Southampton for the Rayleigh studentship, to the Bestway Foundation, Charity No. 297178, UK and to the European Commission Project H2020 CO2EXIDE, for the economic support.The authors acknowledge D.V. Bavykin for useful discussions. The raw data presented in this paper can be found at the repository of the University of Southampton: https://doi.org/10.5258/SOTON/D0530

References

1. Vasconcelos VM, Ponce-de-León C, Nava JL, Lanza MR (2016) Electrochemical degradation of RB-5 dye by anodic oxidation, electro-Fenton and by combining anodic oxidation-electro-Fenton in a filter-press flow cell. J Electroanal Chem 765:179–187
2. Martínez-Huitle CA, Brillas E (2009) Decontamination of wastewaters containing synthetic organic dyes by electrochemical methods: a general review. Appl Catal B Environ 87(3-4):105–145
3. Salazar R, Ureta-Zañartu MS (2012) Mineralisation of triadimefon fungicide in water by electro-Fenton and photo electro-Fenton. Water Air Soil Pollut 223(7):4199–4207
4. Martinez-Huitle CA, Ferro S (2006) Electrochemical oxidation of organic pollutants for the wastewater treatment: direct and indirect processes. Chem Soc Rev 35(12):1324–1340
5. Sandoval MA, Nava JL, Coreño O, Carreño G, Arias LA, Méndez D (2017) Sulfate ions removal from an aqueous solution modeled on an abandoned mine by electrocoagulation process with recirculation. Int J Electrochem Sci 12:1318–1330
6. Salazar R, Garcia-Segura S, Ureta-Zañartu MS, Brillas E (2011) Degradation of disperse azo dyes from waters by solar photoelectro-Fenton. Electrochim Acta 56(18):6371–6379
7. Brillas E, Martínez-Huitle CA (2015) Decontamination of wastewaters containing synthetic organic dyes by electrochemical methods. An updated review. Appl Catal B Environ 166:603–643
8. De Moura DC, Quiroz MA, Da Silva DR, Salazar R, Martínez-Huitle CA (2016) Electrochemical degradation of Acid Blue 113 dye using TiO_2-nanotubes decorated with PbO_2 as anode. Environmental Nanotechnology, Monitoring & Management 5: 13–20
9. Zhou M, He J (2008) Degradation of cationic red X-GRL by electrochemical oxidation on modified PbO_2 electrode. J Hazard Mater 153(1-2):357–363
10. Dos Santos EV, Sáez C, Martínez-Huitle CA, Cañizares P, Rodrigo MA (2015) The role of particle size on the conductive diamond electrochemical oxidation of soil-washing effluent polluted with atrazine. Electrochem Commun 55:26–29
11. Cano A, Cañizares P, Barrera C, Sáez C, Rodrigo MA (2011) Use of low current densities in electrolyses with conductive-diamond electrochemical-oxidation to disinfect treated wastewaters for reuse. Electrochem Commun 13(11):1268–1270
12. Panizza M, Cerisola G (2007) Electrocatalytic materials for the electrochemical oxidation of synthetic dyes. Appl Catal B Environ 75(1-2):95–101
13. De Araújo DM, Sáez C, Martínez-Huitle CA, Cañizares P, Rodrigo MA (2015) Influence of mediated processes on the removal of Rhodamine with conductive-diamond electrochemical oxidation. Appl Catal B Environ 166:454–459
14. Garcia-Segura S, Dos Santos EV, Martínez-Huitle CA (2015) Role of sp_3/sp_2 ratio on the electrocatalytic properties of boron-doped diamond electrodes: a mini review. Electrochem Commun 59:52–55
15. Zhao G, Cui X, Liu M, Li P, Zhang Y, Cao T, Li H, Lei Y, Liu L, Li D (2008) Electrochemical discolouration of refractory pollutant using a novel microstructured TiO_2 nanotubes/Sb-doped SnO_2 electrode. Environ Sci Technol 43:1480–1486
16. Xu M, Wang Z, Wang F, Hong P, Wang C, Ouyang X, Zhu C, Wei Y, Hun Y, Fang W (2016) Fabrication of cerium doped Ti/nanoTiO_2/PbO_2 electrode with improved electrocatalytic activity and its application in organic degradation. Electrochim Acta 201: 240–250
17. Biyoghe BNL, Ibondou MP, Gu X, Xu M, Lu S, Qiu Z, Mbadinga SM (2014) Efficiently synthetic TiO_2 Nano-sheets for PCE, TCE, and TCA degradations in aqueous phase under VUV irradiation. Water Air Soil Pollut 225(5):1951
18. An H, Cui H, Zhang W, Zhai J, Qian Y, Xie X, Li Q (2012) Fabrication and electrochemical treatment application of a microstructured TiO_2-NTs/Sb–SnO_2/PbO_2 anode in the degradation of C.I. Reactive Blue 194 (RB194). Chem Eng J 209:86–93
19. He Z, Huang C, Wang Q, Jiang Z, Chen J, Song S (2011) Preparation of apraseodymium modified Ti/SnO_2-Sb/PbO_2 electrode and its application in the anodic discoluration of the azo dye acid black 194. Int J Electrochem Sci 6:4341
20. Oliveira GR, Fernandes NS, Melo JV, Silva DR, Urgeghe C, Martínez-Huitle CA (2011) Electrocatalytic properties of Ti-supported Pt for decolourizing and removing dye from synthetic textile wastewaters. Chem Eng J 168(1):208–214
21. Cerro-Lopez M, Meas-Vong Y, Méndez-Rojas MA, Martínez-Huitle CA, Quiroz MA (2014) Formation and growth of PbO_2 inside TiO_2 nanotubes for environmental applications. Appl Catal B Environ 100:174–181
22. Frey DA, Weaver HE (1960) NMR Measurements of the Knight Shift in Conducting PbO_2. J Electrochem Soc 107(11):930–932
23. Santos AJD, Xavier DKDS, Silva DRD, Quiroz MA, Martínez-Huitle CA (2014) Use of combined electrochemical approaches for mineralisation and detection of hydroquinone using PbO_2 electrodes. J Mex Chem Soc 58:356–361
24. Martínez-Huitle CA, Panizza M (2010) Application of PbO_2 anodes for wastewater treatment. Advances in chemistry research: applied electrochemistry. Nova Science Publishers Inc., New York
25. Low CTJ, Pletcher D, Walsh FC (2009) The electrodeposition of highly reflective lead dioxide coatings. Electrochem Commun 11(6):1301–1304
26. Savitha R, Raghunathan R, Chetty R (2016) Rutile nanotubes by electrochemical anodisation. RSC Adv 6(78):74510–74514
27. Friedrich J, Ponce-de-León C, Reade G, Walsh FC (2004) Reticulated vitreous carbon as an electrode material. J Electroanal Chem 561:203–217
28. Czerwiński A, Obrębowski RZ, Siwek S, Paleska H, Chotkowski I, Łukaszewski M (2009) RVC as new carbon material for batteries. J Appl Electrochem 39(5):559–567
29. Zhang G, Yang F, Gao M, Fang X, Liu L (2008) Electro-Fenton discolouration of azo dye using polypyrrole/anthraquinonedisulphonate composite film modified graphite cathode in acidic aqueous solutions. Electrochim Acta 53(16):5155–5161
30. Ponce-de-León C, Pletcher D (1995) Removal of formaldehyde from aqueous solutions via oxygen reduction using a reticulated vitreous carbon cathode cell. J Appl Electrochem 25(4):307–314
31. Rodriguez-Valadez F, Ortiz-Éxiga C, Ibanez JG, Alatorre-Ordaz A, Gutierrez-Granados S (2005) Electroreduction of Cr (VI) to Cr (III) on reticulated vitreous carbon electrodes in a parallel-plate reactor with recirculation. Environ Sci Technol 39(6):1875–1879
32. Reade GW, Nahle AH, Bond P, Friedrich JM, Walsh FC (2004) Removal of cupric ions from acidic sulfate solution using reticulated vitreous carbon rotating cylinder electrodes. J Chem Technol Biotechnol 79(9):935–945
33. Hossein M, Momeni MM (2012) Preparation and characterisation of TiO_2 nanotubular arrays for electro-oxidation of organic compounds: effect of immobilisation of the noble metal particles. Int J Mod Phys 5:41–48
34. Simond O, Comninellis C (1997) Anodic oxidation of organics on Ti/IrO_2 anodes using Nafion® as electrolyte. Electrochim Acta 42(13-14):2013–2018

35. Ramírez G, Recio FJ, Herrasti P, Ponce-de-León C, Sirés I (2016) Effect of RVC porosity on the performance of PbO_2 composite coatings with titanate nanotubes for the electrochemical oxidation of azo dyes. Electrochim Acta 204:9–17
36. Jaeger CD, Bard AJ (1979) Spin trapping and electron spin resonance detection of radical intermediates in the photodecomposition of water at TiO_2 particulate systems. J Phys Chem 83(24):3146–3152
37. Naccache C, Meriaudeau P, Che M (1971) Identification of oxygen species adsorbed on reduced titanium dioxide. Trans Faraday Soc 67:506–512
38. Fukuzawa S, Sancier KM, Kwan T (1968) Photoadsorption and photodesorption of oxygen on titanium dioxide. J Catal 11(4): 364–369
39. Wang Y, Shi R, Lin J, Zhu Y (2010) Significant photocatalytic enhancement in methylene blue discolouration of TiO_2 photocatalyst via graphene-like carbon in situ hybridisation. Appl Catal B Environ 100(1-2):179–183
40. Lawless D, Serpone N, Meisel D (1991) Role of $^{\bullet}OH$ radicals and trapped holes in photocatalysis. A pulse radiolysis study. J Phys Chem 95(13):5166–5170
41. Muneer MB, Qamar D, Tariq M, Faisal MA (2005) Photocatalysed reaction of few selected organic systems in presence of titanium dioxide. Appl Catal A Gen 289(2):224–230
42. Sasaki T, Watanabe M (1998) Osmotic swelling to exfoliation exceptionally high degrees of hydration of a layered titanate. J Am Chem Soc 120(19):4682–4689
43. Grey IE, Li C, Madsen IC, Watts JA (1987) The stability and structure of Cs_x $[Ti_2\text{-}x_4\square x_4]O_4$, $0.61 < x < 0.65$. J Solid State Chem 66(1):7–19
44. Recio FJ, Herrasti P, Sirés I, Kulak AN, Bavykin DV, Ponce-de-León C, Walsh FC (2011) The preparation of PbO_2 coatings on reticulated vitreous carbon for the electro-oxidation of organic pollutants. Electrochim Acta 56(14):5158–5165
45. Sirés I, Low CTJ, Ponce-de-León C, Walsh FC (2010) The characterisation of PbO_2-coated electrodes prepared from aqueous methanesulfonic acid under controlled deposition conditions. Electrochim Acta 55(6):2163–2172
46. Kim SJ, Yun YU, Oh HJ, Hong SH, Roberts CA, Routray K, Wachs IE (2010) Characterisation of hydrothermally prepared titanate nanotube powders by ambient and in situ Raman spectroscopy. J Phys Chem Lett 1(1):130–135
47. Hsueh CL, Huang YH, Wang CC, Chen CY (2005) Photoassisted Fenton discolouration of nonbiodegradable azo-dye (reactive black 5) over a novel supported iron oxide catalyst at neutral pH. J Mol Catal A 245:78–86
48. Jafari N, Kasra-Kermanshahi R, Soudi MR, Mahvi AH, Gharavi S (2012) Degradation of a textile reactive azo dye by a combined biological-photocatalytic process: *Candida tropicalis* Jks2 -TiO_2/Uv. Iranian J Environ Health Sci Eng 9(1):33
49. Sugiyana D, Handajani M, Kardena E, Notodarmojo S (2014) Photocatalytic degradation of textile wastewater containing reactive black 5 azo dye by using immobilized TiO_2 nanofiber-nanoparticle composite catalyst on glass plates. Journal of JSCE 2(1):69–76
50. Notodarmojo S, Sugiyana D, Handajani M, Kardena E, Larasati A (2017) Synthesis of TiO_2 nanofiber-nanoparticle composite catalyst and its photocatalytic decolourisation performance of reactive black 5 dye from aqueous solution. J Eng Technol Sci 49(3):340–356
51. Muruganandham M, Sobana N, Swaminathan M (2006) Solar assisted photocatalytic and photochemical degradation of Reactive Black 5. J Hazard Mater 137(3):1371–1376
52. Lucas MS, Peres JA (2006) Decolourisation of the azo dye reactive black 5 by Fenton and photo-Fenton oxidation. Dyes Pigments 71: 235–244
53. Mahmoodia NM, Arami M, Limaee NY, Tabrizi NS (2005) Decolourisation and aromatic ring discolouration kinetics of direct red 80 by UV oxidation in the presence of hydrogen peroxide utilizing TiO_2 as a photocatalyst. Chem Eng J 112(1-3):191–196
54. Jiang Y, Wang WN, Biswas P, Fortner JD (2014) Facile aerosol synthesis and characterisation of ternary crumpled graphene-TiO_2-magnetite nanocomposites for advanced water treatment. ACS Appl Mater Interfaces 6(14):11766–11774
55. Ilisz I, Laszlo Z, Dombi A (1999) Investigation of the photodecomposition of phenol in near-UV-irradiated aqueous TiO2 suspensions. I: effect of charge-trapping species on the discolouration kinetics. Appl Catal A Gen 180:25–33
56. Iwaszuk A, Nolan M (2013) Lead oxide-modified TiO_2 photocatalyst: tuning light absorption and charge carrier separation by lead oxidation state. Catal Sci Technol 3(8):2000–2008